

6H-SiC Photoconductive Switches Triggered at Below Bandgap Wavelengths

J.S.Sullivan and J.R. Stanley
University of California
Lawrence Livermore National Laboratory
Livermore, CA 94550

Abstract-Semi-insulating Silicon Carbide (SiC) is an attractive material to use to construct high voltage, compact, photoconducting semiconductor switches (PCSS) due to its large bandgap, high critical electric field strength, high electron saturation velocity, and high thermal conductivity. The critical field strength of 3 MV/cm of 6H-SiC makes it particularly attractive for compact, high voltage, fast switching applications such as a Dielectric Wall Accelerator (DWA). To realize the benefits of the high bulk electric field strength of SiC and diffuse switch current, carriers must be excited throughout the bulk of the photo switch. Photoconducting switches with opposing electrodes were fabricated on “a” plane, Vanadium compensated, semi-insulating, 6H-SiC substrates. The PCSS devices were switched by optically exciting deep extrinsic levels lying within the 6H-SiC bandgap. The SiC photoswitches were tested up to a bias voltage of 11000 V with a corresponding peak current of 150 A. The 6H-SiC substrates withstood average electric fields up to 27 MV/m. Minimum PCSS dynamic resistances of 2 and 10 Ohms were obtained with 13 mJ optical pulses at 532 and 1064 nm wavelengths, respectively.

I. INTRODUCTION

The 6H-SiC polytype has a wide band-gap (3 eV), high critical field strength (3 – 4 MV/cm), high saturated electron velocity (2.0×10^7 cm/s), and high thermal conductivity (4.9 W/cm °C). These material properties make semi-insulating 6H-SiC an attractive semiconductor material for the Photoconductive Semiconductor Switch (PCSS) application. Previous SiC PCSS work [1,2,3] used high resistivity, low impurity SiC polytypes and focused on lateral geometry surface switches that used above band-gap wavelengths of light to trigger the switches. Lateral geometry surface PCSS are limited by surface flashover, surface carrier mobility, and high current density. PCSS with opposing electrical contacts deposited on Vanadium compensated, semi-insulating, 6H-SiC substrates can be triggered using below band-gap light to excite carriers from extrinsic levels throughout the bulk of the material. This results in diffuse photocurrent and switch hold off voltages determined by the bulk breakdown field strength of 6H-SiC. The bulk switching capability and semi-insulating nature of 6H-SiC are enabled by the addition of the dopant, Vanadium. Vanadium is an amphoteric impurity that can act as a deep acceptor, or a deep donor. The local Fermi level in the 6H-SiC is determined by the relative densities of the impurities, nitrogen and boron, that are normally found in the

material. Vanadium acts as a deep acceptor when the Nitrogen impurity density sufficiently exceeds the boron impurity density, which is the case for the 6H-SiC material we have tested. Another feature of this material is that the Fermi level will be pinned close to the Vanadium acceptor level. The deep (0.7 eV below conduction band) Vanadium acceptor levels accept electrons donated from the shallow (0.08 eV below conduction band) nitrogen donor levels, resulting in semi-insulating 6H-SiC material. The electrons residing in the extrinsic Vanadium acceptor levels can be excited into the conduction band by photons with energies exceeding 0.7 eV.

II. EXPERIMENT

Four PCSS devices were fabricated from samples of 400 μm thick, 1.2 cm per side, square substrates of “a” plane, Vanadium compensated, semi-insulating 6H-SiC. The four facets of the substrate were polished to enhance optical coupling into the bulk of the substrate. The contacts consist of a 1cm diameter, circular metalization centered on opposing sides of the substrate. The metalization formed an ohmic contact and consisted of layers of nickel, titanium, platinum, and gold. The metal deposition and anneal were performed at SemiSouth Laboratories Inc. in Starksville, MS. Indium coated copper electrodes were brazed to the substrate metalizations to facilitate electrical connection. The finished 6H-SiC PCSS assembly is shown in Figure 1. The 6H-SiC PCSS assembly was prepared for photoconductivity measurements by cleaning the PCSS facets to remove any organic residue. All four PCSS facets were inspected by microscope and given identification marks prior to photoconductivity tests. Photoconductivity tests were performed using 1064 nm and frequency doubled 532 nm wavelength light from a Q-switched Nd:YAG laser with an 8 ns FWHM output pulse. The optical pulse was focused and aligned to obtain as uniform as possible light pulse over a rectangular area measuring 1 cm wide by 400 μm high. The optical pulse was then centered on the PCSS facet. Photoconductivity tests were performed using optical pulse energies ranging from 1 to 14 mJ. The optical energy was increased in 1 mJ increments using a polarizer-waveplate pair. PCSS facets were inspected for damage by microscope between optical pulse energy increments. The

Report Documentation Page

Form Approved
OMB No. 0704-0188

Public reporting burden for the collection of information is estimated to average 1 hour per response, including the time for reviewing instructions, searching existing data sources, gathering and maintaining the data needed, and completing and reviewing the collection of information. Send comments regarding this burden estimate or any other aspect of this collection of information, including suggestions for reducing this burden, to Washington Headquarters Services, Directorate for Information Operations and Reports, 1215 Jefferson Davis Highway, Suite 1204, Arlington VA 22202-4302. Respondents should be aware that notwithstanding any other provision of law, no person shall be subject to a penalty for failing to comply with a collection of information if it does not display a currently valid OMB control number.

1. REPORT DATE 01 MAY 2006	2. REPORT TYPE N/A	3. DATES COVERED -	
4. TITLE AND SUBTITLE 6H-SiC Photoconductive Switches Triggered at Below Bandgap Wavelengths		5a. CONTRACT NUMBER	
		5b. GRANT NUMBER	
		5c. PROGRAM ELEMENT NUMBER	
6. AUTHOR(S)		5d. PROJECT NUMBER	
		5e. TASK NUMBER	
		5f. WORK UNIT NUMBER	
7. PERFORMING ORGANIZATION NAME(S) AND ADDRESS(ES) University of California Lawrence Livermore National Laboratory Livermore, CA 94550		8. PERFORMING ORGANIZATION REPORT NUMBER	
9. SPONSORING/MONITORING AGENCY NAME(S) AND ADDRESS(ES)		10. SPONSOR/MONITOR'S ACRONYM(S)	
		11. SPONSOR/MONITOR'S REPORT NUMBER(S)	
12. DISTRIBUTION/AVAILABILITY STATEMENT Approved for public release, distribution unlimited			
13. SUPPLEMENTARY NOTES See also ADM001963. IEEE International Power Modulator Symposium (27th) and High-Voltage Workshop Held in Washington, DC on May 14-18, 2006, The original document contains color images.			
14. ABSTRACT			
15. SUBJECT TERMS			
16. SECURITY CLASSIFICATION OF:			17. LIMITATION OF ABSTRACT
a. REPORT unclassified	b. ABSTRACT unclassified	c. THIS PAGE unclassified	UU
			18. NUMBER OF PAGES 4
			19a. NAME OF RESPONSIBLE PERSON

photoconductivity of the PCSS was measured using the circuit shown in Figure 2. The 1.5 μF capacitor of the test

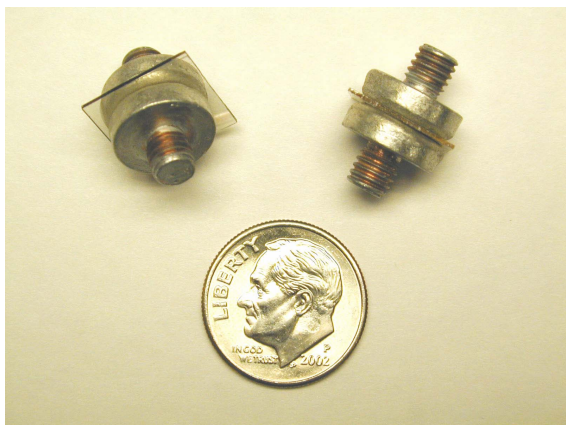


Fig. 1. Vanadium compensated, semi-insulating, 6H-SiC PCSS assembly

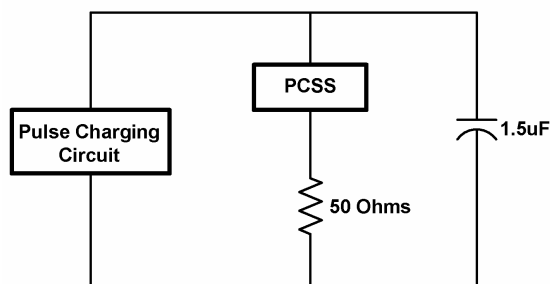


Fig. 2. Simple schematic for PCSS photoconductivity test circuit

circuit was pulse charged to bias voltages ranging from 250 volts to 4.25 kV in 30 μs . The PCSS was optically triggered after a 30 μs flat top interval of the pulse bias voltage. The voltage across the PCSS was measured differentially and the PCSS current was measured by monitoring the voltage across a 50-Ohm load resistor in series with the PCSS. The PCSS voltage and current for a charge voltage of 4.25 kV and optical pulse energy of 13 mJ at 1064 nm are shown in Figure 3. The PCSS voltage starts at 4.25 kV and collapses to approximately 750 Volts in 10 ns, while the PCSS current increases from zero to 70 Amps. The PCSS current pulse is similar in temporal profile to the 1064 nm optical trigger pulse. However, the photocurrent has a 16 ns FWHM pulse-width indicating a carrier recombination time of a few nanoseconds, or less. The minimum dynamic PCSS resistance for the pulse shown in Figure 3 is 11 Ω . The minimum dynamic PCSS resistance is approximately constant for fixed optical pulse energy, regardless of the charge voltage. The minimum dynamic PCSS resistance as a function of optical pulse energy at 1064 and 532 nm is shown in Figure 4. The minimum dynamic PCSS resistance decreases rapidly with optical pulse energy for both optical wavelengths. The PCSS attains a lower minimum dynamic resistance at all optical energies for excitation with 532 nm

light compared to excitation with 1064 nm light. This is a result of charge carriers being excited from additional extrinsic levels by the 532 nm wavelength.

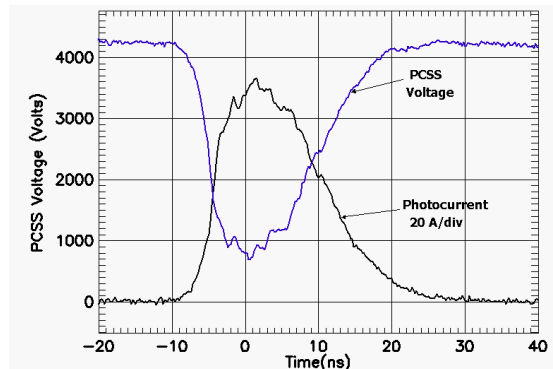


Fig. 3. PCSS voltage and current for bias voltage of 4.25 kV and 13 mJ optical trigger at 1064 nm

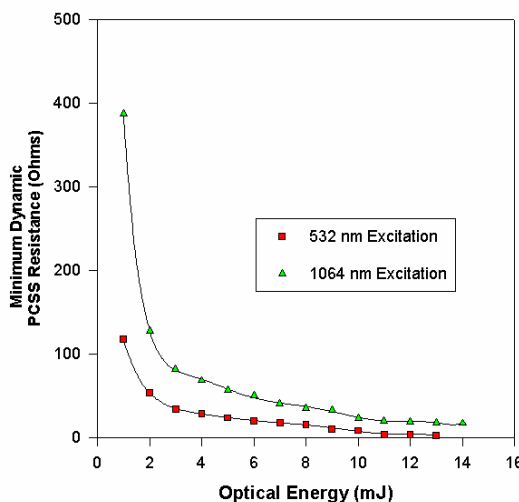


Fig. 4. Minimum dynamic PCSS resistance as function of optical trigger energy for 532 and 1064 nm.

The dark current of the PCSS was measured while applying a dc bias using a picoammeter electrically in series with the PCSS. The voltage across the PCSS was monitored with a precision (1%) 1000 M Ω , resistive divider. The dark current varied linearly with the dc bias voltage and ranged from a small fraction of a nanoampere up to 5.8 nA at the highest dc bias of 1000 volts, as shown in Figure 5. The PCSS dark resistance and resistivity were calculated to be 170 G Ω and 3.2X10¹² Ω -cm using the dark current data. The ratio of the dark resistance to the minimum dynamic PCSS resistance of Figure 4 (2 Ω) is 8.5x10¹⁰. The resistivity has been reduced by almost eleven orders of magnitude by exciting extrinsic levels in the bulk of the Vanadium compensated 6H-SiC.

The peak photocurrent in the PCSS has been measured as a function of bias voltage and optical pulse energy for both 532 and 1064 nm wavelengths. The peak photocurrent varies linearly with the bias voltage for fixed optical pulse energy as

shown in Figure 6. The slope of the linear variation of peak photocurrent with bias voltage decreases when the fixed optical pulse energy is reduced. This is what should be expected since we are optically modulating the PCSS resistance.

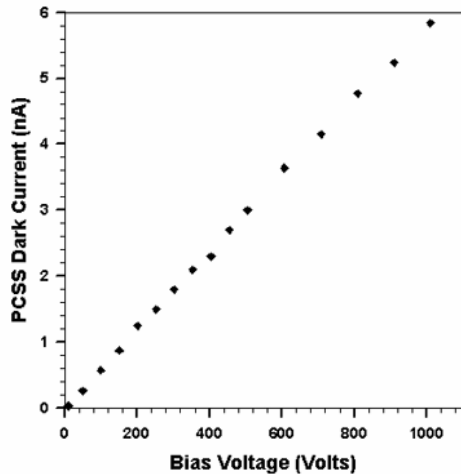


Fig. 5. Variation of PCSS dark current with bias voltage.

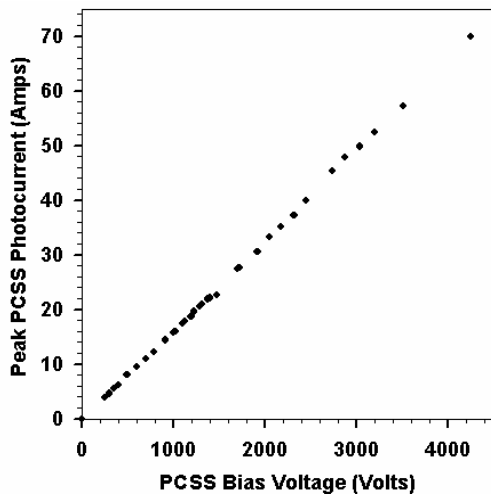


Fig. 6. Peak PCSS photocurrent versus bias voltage for 13 mJ optical excitation at 1064 nm.

The saturation of the peak PCSS photocurrent with increasing optical pulse energy for fixed bias voltage of 750 volts is shown in Figure 7. The peak PCSS photocurrent for illumination with 532 nm was consistently 3 – 4 Amps higher than the peak photocurrent obtained with 1064 nm illumination for this PCSS. This is a result of the 532 nm wavelength (2.33 eV) exciting more extrinsic levels than the 1064 nm wavelength (1.17 eV). A consistent difference in peak PCSS photocurrent with excitation wavelength was observed in all the PCSS devices tested. However, the magnitude of the difference in peak PCSS photocurrent for different excitation wavelengths varied from 2 Amps up to 6 Amps. A possible explanation for variation of the difference

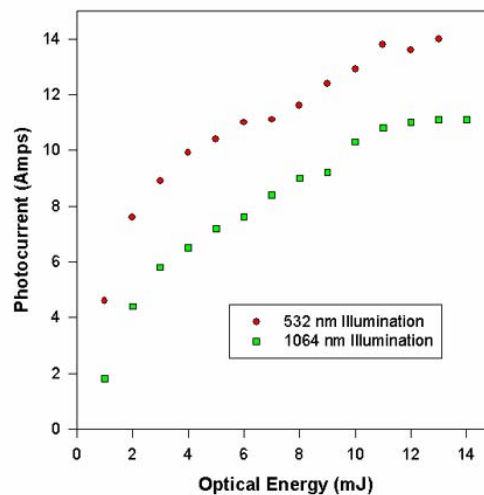


Fig. 7. Peak PCSS photocurrent versus optical excitation energy for 750 Volt bias.

in peak photocurrent for different PCSS devices is that the PCSS substrates are cut from the a-plane of the 6H-SiC crystal. The sections that were originally cut from the 6H-SiC crystal measured 3.6 cm in the crystal growth (c) direction. The sections were then cut into 1.2 cm long substrates. We would expect variation in substrate impurity densities along the growth direction because the impurity densities usually decrease during crystal growth. We expect somewhat different performances from substrate to substrate since we are exciting carriers from extrinsic (impurity) levels.

The nature of some of the different extrinsic levels being excited at the 1064 and 532 nm optical wavelengths is illustrated in Figure 8. The PCSS photocurrents for 11 mJ optical excitation at 532 and 1064 nm wavelengths show a significant difference in amplitude and pulse shape. The most notable difference is the long tail on the photocurrent excite at 532 nm. The current tail persists and slowly decays to zero in approximately one millisecond.

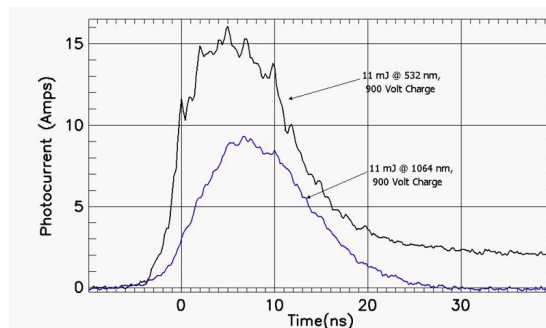


Fig. 8. PCSS photocurrent temporal pulse for 11 mJ optical excitation at 532 and 1064 nm wavelengths.

We believe electron traps due to crystal defects located 1.3 – 1.6 eV below the conduction band are contributing to the carriers in the photocurrent tail. Electrons are captured by the traps and thermally excited back into the conduction band resulting in a long decay time. The electron trap level has a

recovery time of 200 μ s. It also appears that the electron traps are filled prior to optical excitation based on the much faster rate of rise of photocurrent excited at 532 nm. However, the electron trap level contributes only 2 of 15 Amps peak photocurrent at 532 nm. We should expect that the electrons excited from Vanadium acceptor level, that we believe constitutes the entire photocurrent at 1064 nm, will also be excited at 532 nm. There appears to be at least a third component of photocurrent with a rapid rise and decay time that is present in the photocurrent at 532 nm. We believe that the additional carriers are holes being excited into the valence band from Vanadium acceptor levels that have not been ionized. A significant fraction of Vanadium acceptor levels is not ionized because the Fermi level is pinned close to the Vanadium acceptor level. In addition, Vanadium acceptor levels are returned to the neutral state after electrons that they had captured are excited into the conduction band. Electrons can be excited from the valence band into the neutral Vanadium acceptor levels that lie 2.3 eV above the valence band by 532 nm (2.33 eV) wavelength light. Electrons that are excited into the neutral Vanadium acceptor levels leave holes in the valence band that contribute to the conduction current of the PCSS.

A single PCSS device was tested to electrical failure of the 6H-SiC substrate. The charge circuit was modified to produce a 3 μ s risetime. The load resistor was reduced to 9 Ohms. The 1064 nm, 9 mJ, optical pulse was applied after a 5 μ s flat top interval of the pulse bias voltage. The PCSS device was submerged in a transparent liquid dielectric to prevent tracking around the edge of the device. The PCSS failed after conduction at a pulsed bias voltage of 11 kV. This voltage level represents an average field of 27.4 MV/m in the 6H-SiC substrate. Failure occurred through the bulk of the substrate directly under the edge of the device metalization, the location of greatest electric field enhancement. A peak field of 200 MV/m was numerically calculated for the failure point from the geometry of the failed device. We believe that making use of oxide coatings and SiC etching techniques will allow for PCSS device operations at significantly higher average electric fields.

The four PCSS devices that were tested fell into one of two categories based on minimum switch resistance. Three devices achieved a minimum dynamic on resistance of 10 - 11 Ohms at 13 mJ optical trigger at 1064 nm. The remaining device had minimum dynamic on resistance of 2 - 3 Ohms at optical trigger energies of 13 mJ at 1064 nm. There was no apparent difference in the switch facets. The density of the Vanadium (V), Nitrogen (N), Boron (B), and Aluminum (Al)

impurities were measured using Secondary Ion Mass Spectroscopy (SIMS) for the “low” resistance switch and one of the three “high” resistance switches. The Al density was so low as to be negligible. The low resistance switch substrate had a higher density of N and lower density of V and B than the high resistance switch substrate. The lower resistance was attributed to the higher N density. The Vanadium acceptor levels trap the electrons donated by the N levels. These are the electrons that are excited into the conduction band. The more electrons trapped by the Vanadium acceptor levels, the lower the on resistance. The impurity density measurements have indicated a path toward optimizing the impurity levels in the Vanadium compensated, 6H-SiC.

In conclusion, bulk PCSS have been constructed from a-plane, Vanadium compensated, semi-insulating 6H-SiC. The PCSS were switched on by optically exciting charge carriers from extrinsic levels using 532 and 1064 nm wavelength light. Operation in this manner allows for diffuse current conduction and the ability to take advantage of the high breakdown electric field of the bulk 6H-SiC material. PCSS resistance was reduced from 170 G Ω to 2 and 11 Ω by applying 13 mJ optical energy pulses at 532 and 1064 nm wavelengths, respectively. Photoconductivity measurements were performed to a bias voltage level of 4.25 kV corresponding to an average electric of 10 MV/m between PCCS contacts. A slowly decaying current component with a 200 μ s recombination time was observed for 532 nm wavelength excitation. A single PCSS was tested to electrical failure at an average field of 27.4 MV/m in the 6H-SiC substrate. The failure occurred at the point of highest electric field enhancement. We will utilize material processing techniques to achieve higher field operation of the PCSS devices. This initial work indicates that a compact, high voltage, high current switch can be developed from exciting the extrinsic levels in Vanadium compensated, 6H-SiC substrates.

REFERENCES

- [1] S. Dogan et al., “4H-SiC photoconductive switching devices for use in high-power applications,” *Applied Physics Letters*, vol. 82, pp. 3107-3109, May 2003.
- [2] S. Sheng, M. Spencer, X. Tang, P. Zhou, and G. Harris, “Polycrystalline cubic silicon carbide photoconductive switch,” *IEEE Electron Device Letters*, vol. 18, pp 372-374, August 1997.
- [3] K. Zhu et al., “Effect of n⁺-GaN subcontact layer on 4H-SiC high-power photoconductive switch,” *Applied Physics Letters* 86, p. 261108, June, 2005.
- [4] P. Cho, J. Goldhar, C. Lee, S. Sadow, and P. Neudeck, “Photoconductive and photovoltaic response of high-dark-resistivity 6H-SiC devices,” *Journal of Applied Physics*, vol. 77, pp. 1591-1599, Feb. 1995.